

# Analysis of inertia, damping, and synchronization characteristics in grid-connected photovoltaic systems with fuzzy logic control

Mimmithi Bhanu Prakash, Pradosh Ranjan Sahoo

School of Electronics Engineering, Vellore Institute of Technology-Andhra Pradesh University, Andhra Pradesh, India

## Article Info

### Article history:

Received Jun 15, 2023

Revised Jan 1, 2024

Accepted Jan 18, 2024

### Keywords:

Direct current-direct current converter

Droop controller

Fuzzy logic controller

Maximum power point tracking controller

Proportional integral controller

Solar photovoltaic

## ABSTRACT

The integration of renewable energy sources (RES) into DC-distributed power systems (DC-DPSS) is gaining traction as a sustainable energy solution. However, the inherent variability of RES output can introduce instability into the grid, posing challenges for maintaining system reliability and stability. Fuzzy logic controllers (FLCs) have emerged as a promising approach to mitigate these instability issues, offering a robust and adaptable control strategy that can effectively handle the complexities of DC-DPSS. This paper examines the application of FLCs in DC-DPSS, exploring their effectiveness in addressing instability caused by RES fluctuations. FLCs are a control system that leverages fuzzy logic, a form of logic that utilizes linguistic variables to represent uncertainty, make decisions, and improve the stability of DC-distributed power systems. The research analyzes various system parameters, including inertia, damping, and synchronization characteristics, using a static synchronous generator (SSG) model. The study builds upon prior findings by adding a fuzzy logic controller to the existing system. The results showed better performance which resulted in improved inertia, damping, and synchronization characteristics. The efficiency of the proposed controller is demonstrated using MATLAB/Simulink.

This is an open access article under the [CC BY-SA](https://creativecommons.org/licenses/by-sa/4.0/) license.



## Corresponding Author:

Pradosh Ranjan Sahoo

School of Electronics Engineering, Vellore Institute of Technology-Andhra Pradesh University

VIT-AP University, G-30, Inavolu, Beside AP Secretariat Amaravati, Guntur 522237, Andhra Pradesh, India

Email: pradosh.sahoo@vitap.ac.in

## 1. INTRODUCTION

In recent years, demand of renewable energy sources for power generation has increased due to its least effect of environmental pollution [1]. Therefore, grid tied photovoltaic (PV) power generation system has shown an explosive growth as one of the sources for clean energy. In order to keep the direct current (DC) bus voltage stable and distribute the load evenly across the converters, a new droop control method that adjusts the value of the droop resistance based on load requirement is suggested in [2]. Local load and line resistance also have a role in determining the voltage distribution. In [3], [4] the growth of the wind power industry has affected the supply and design of the electricity grid. By working in sync with the electricity grid, wind turbines with grid-forming control prevent phase-locked loops. Here, they examined the grid-forming doubly fed induction generator (DFIG's) modeling, inertia, and damping under a variety of operational conditions. The simulation results demonstrate a link between inertia and damping in various operational scenarios. In [5], it is analyzed that by controlling the power retained by capacitors on the direct current side, the droop control of a rate of change of frequency (RoCoF) helps to dampen frequency fluctuations that can cause problems and also classifies the control time-frame and inertia which helps in

reducing the frequency variation. The study [6] addresses frequency control challenges in micro-grids caused by erratic renewable energy source (RES) outputs. It proposes integrating a fuzzy logic-based integral controller and a superconducting magnetic energy storage (SMES) unit to mitigate these fluctuations. Using MATLAB/Simulink simulations, the system's performance is evaluated, revealing that this combined setup outperforms conventional integral controller-based systems. Specifically, the fuzzy logic-based integral controller with the SMES unit effectively dampens frequency oscillations arising from abrupt load changes and intermittent RES behavior, showcasing enhanced dynamic performance and superior frequency stability within the micro-grid. Tekin *et al.* [7] introduced a novel switched capacitor-based quadratic boost converter (QBC) integrated with fuzzy logic control (FLC) for efficient integration of low-power renewable energy sources (RESs) like photovoltaic arrays with the grid. The proposed converter yields higher voltage gain at low duty cycles compared to traditional converters, enhancing voltage stress reduction across the main power switch for increased reliability and durability. By employing a switched-capacitor topology, this system minimizes voltage and current stresses on power switches and diodes, improving efficiency. Mathematical analysis and MATLAB/Simulink simulations validate the effectiveness. Sumarmad *et al.* [8] described microgrids as a renewable energy solution for climate change, operating connected or independently. It highlights the role of energy storage in stability and proposes three smart controllers for efficient microgrid management. MATLAB Simulink simulations favor the fuzzy logic controller for its effectiveness. The study emphasizes stability enhancement under diverse load and solar conditions, stressing the controllers' success in ensuring safe microgrid operation. Future plans involve experimental validation and integrating energy optimization into the system. The study [9] suggested a new way to improve a small self-sufficient power grid using wind and diesel generators, along with batteries for efficiency. An intelligent energy management system (IEMS) was made in two steps: first, using extra energy when wind is low or demand is high, and second, using smart controls to boost performance. Tests showed that both methods keep the grid balanced and improve power stability, with the 3D-fuzzy logic-frequency regulation (3D-FL-FR) control slightly outperforming ANN, ensuring steady power even with high demand or changing wind.

In [10]–[12], it was observed that virtual synchronous generator (VSG) regulates the inverter of a distributed generating unit to maintain power system reliability. Virtual inertia is also expressed by the swing equation of a synchronous machine. Active and reactive power can be regulated using droop control or a VSG, having advantages of virtual inertia and simulating swing equation. Variations in the swing equation are investigated by comparing the two control methods in real-time. In [13], [14], the fundamentals, major characteristics, application concerns, and development trends of voltage source controller VSC-dominated power system modeling and stability analysis techniques are discussed. A novel controller is developed in [15], [16] to improve the microgrid's frequency response to disturbances such as large frequency deviations. The various variables in the proposed control's design are discussed as well. It was also stated that the grid-connected power converters were used as a method for implementing the idea of virtual inertia in a distributed power system. In [17] static synchronous generator (SSG) is introduced to examine SSG dynamics and stability, which may be compared to those of pulse width modulation (PWM) inverters due to their shared physical mechanisms and mathematical models. This study addresses challenges in maximizing solar power generation due to module mismatching and partial shading issues. Existing Maximum Power Point Tracking (MPPT) techniques, while effective in stable conditions, often struggle with speed and precision. To overcome these limitations, the paper proposes a novel combinatorial MPPT algorithm based on fuzzy logic control and an improved farmland fertility optimization (IFFO) method. This approach optimizes controller parameters, demonstrating superior performance in both uniform irradiance and partial shading scenarios compared to six other methods. The proposed algorithm achieves efficiencies of 99% for various conditions, ensuring optimal solar power generation [18].

This research explores the risks of unexpected shifts between grid-connected (GC) and stand-alone (SA) modes in distributed generation systems. It proposes a fuzzy logic (FL)-based approach to enable a controlled, smooth transition between modes, avoiding sudden state variable changes that could damage the system. Fuzzy logic algorithm (FLA) generates a gradual trajectory from GC to SA modes using unified control, enhancing voltage loop control for better disturbance rejection. Simulation tests validate the efficacy of the FL-based strategy, offering a resilient approach for safer mode transitions in distributed generation systems [19]. Inertia, damping, and synchronization characteristics of a solar grid-tied and inverter-side DC voltage droop control system using the SSG mathematical model, and the electrical torque analysis technique were examined. Problems related to power quality issues, angular stability, voltage stability and various other technical aspects were also discussed in [20]–[22]. FLC is a specialized method of control that differs from traditional controllers like the proportional integral (PI) controller. It is like using a smart and adaptable approach to managing a system.

In our research, instead of sticking with the usual PI controller, we decided to explore the possibilities offered by FLC. To do this, we looked at past studies to understand what really matters when it

comes to making a system perform its best. Specifically, we made significant enhancements in how our system handles inertia (which is how resistant it is to change), damping (which reduces unwanted movements), and synchronization (making sure everything works together smoothly). These improvements have propelled our system to a new level of efficiency and performance. It is not just about technology; it is a significant step forward in making renewable energy sources work seamlessly with the electrical grid. This research brings us closer to a more reliable and efficient future for renewable energy integration. In section 2 the paper deals with the system configuration followed by system dynamic characteristics analysis in section 3. In section 4 the paper gives brief about fuzzy logic controller and in section 5 the simulation results were shown. In section 6 the conclusion of the paper is presented.

**2. SYSTEM CONFIGURATION**

The schematic representation of grid connected PV power generation system with DC voltage droop control is shown in Figure 1. A solar module, a grid-tied inverter that makes use of DC voltage droop control, and a DC/DC converter that operates under maximum power point tracking control make up the components of this system. The maximum power point tracking (MPPT) feature of the DC/DC converter makes it possible to have accurate control over the voltage drop on the side of the DC capacitor and the frequency fluctuation on the side of the inverter. In general, the purpose of this system is to generate power from the solar module in a reliable manner, transmit that electricity to the grid, and maintain a steady voltage and frequency during the entirety of its operation.

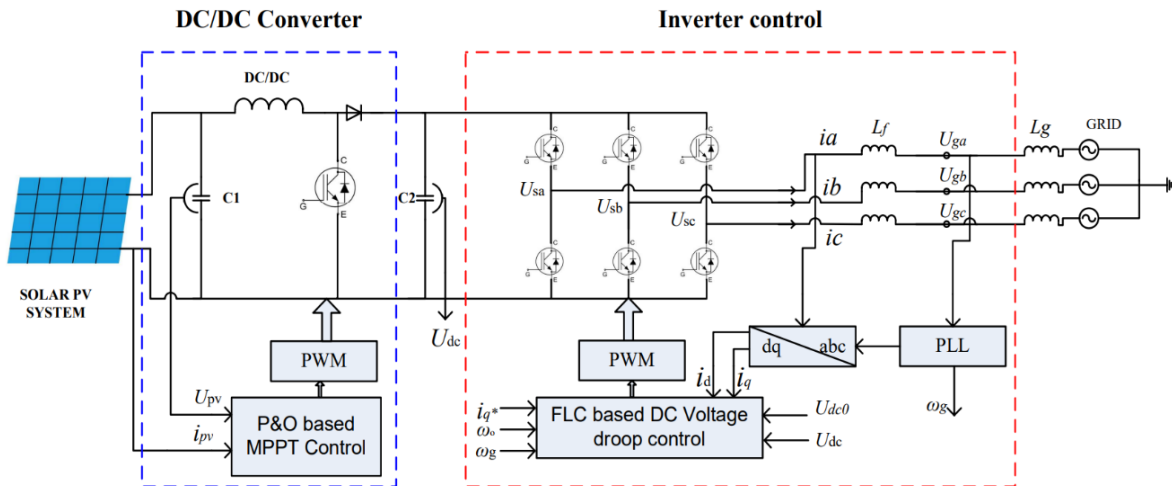


Figure 1. Main circuit diagram

**2.1. Solar PV system**

The mathematical equation shown in (1) can be used for the analysis of power generation in solar PV system.

$$P = \eta * A * G * PR \tag{1}$$

Where  $P$  is power output in watts ( $W$ ),  $\eta$  is panel efficiency,  $A$  is the panel area in square meters ( $m^2$ ),  $G$  is the solar irradiance in watts per square meter ( $W/m^2$ ), and  $PR$  is the performance ratio (a factor that accounts for various losses such as temperature, shading, and soiling). The charge controller can be modelled by (2).

$$V_c = V_{mp} - \left(\frac{I}{I_{mp}}\right) * (V_{mp} - V_{oc}) \tag{2}$$

Where  $V_c$  stands for the regulated voltage, maximum voltage and current of PV is shown with  $V_{mp}$  and  $I_{mp}$ ,  $I$  for the current leaving the panel, and  $V_{oc}$  for its open-circuit voltage.

## 2.2. Boost converter

PV power is inefficient for most loads since it generates less power. Thus, a step-up converter boosts PV levels. This is important because the DC-DC converter or inverter's input voltage is fixed, but the PV panel's output voltage varies with sunshine. A boost converter allows energy to flow efficiently between solar panels and converters, maximizing power generation.

The external structure of photovoltaic module is represented by the reference voltage and current signals and at DC side are represented with  $U_{pv}^*$  and  $I_{pv}^*$ ,  $U_{pv}$  and  $I_{pv}$  are voltage and current output by pv module respectively. These reference signals are fed into a proportional integral (PI) controller as input as shown in Figure 2. Double closed-loop controller [23] consisting of an outer voltage loop and an inner current loop at DC side, is present in the boost DC/DC converter.

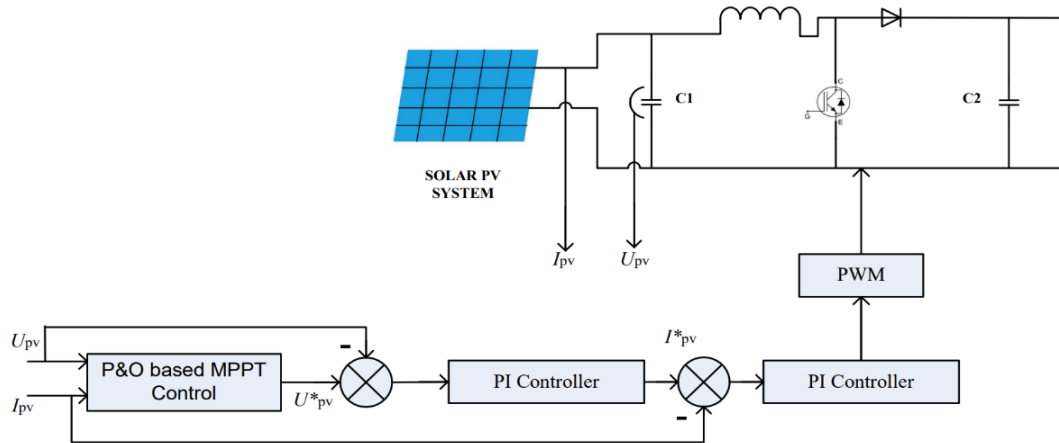


Figure 2. Controlling topology of boost converter

In the DC voltage time scale, the dynamic process of inner current loop is ignored. Thereby the output current of the PV is expressed in (3).

$$I_{pv}^* = I_{pv} = (K'_p) + \frac{K_i}{s} (U_{pv}^* - U_{pv}) \quad (3)$$

The outer voltage loop is characterized by its proportional and integral coefficients, which are identified as  $K'_p$  and  $K_i$ , respectively. The photovoltaic module produces its greatest amount of power when operating in conditions of constant temperature and constant light intensity. Both DC/DC converter and the photovoltaic module's output power are constant at this operating point. Consequently, it is clear that:

$$\Delta P_{in} = 0 \quad (4)$$

## 2.3. Grid-tied inverter

A grid-connected converter may return AC electricity from renewable sources like solar panels to the grid. The inverter's AC output is matched to the utility grid's AC voltage and frequency by a power conditioning unit (PCU). Voltage regulation maintains the inverter's AC output voltage at the grid voltage, preventing voltage fluctuations that could harm equipment or poor power quality. Power factor correction corrects the system's current-voltage imbalance, improving efficiency. Here decoupling prevents grid frequency variations. Figure 3 shows the grid connected mode of inverter side and can be derived as (5).

$$I_d^* = I_d = -(U_{dc}^* + U_{dc0} - U_{dc}) \left( K_p + \frac{K_i}{s} \right) \quad (5)$$

where current in d-axis and q-axis in the  $dq$  coordinate system was given by  $I_d$  and  $I_q$ . The q-axis current reference value is represented by  $I_q^*$  and d-axis current reference value is represented by  $I_d^*$ . Proportional coefficient  $K_p$  and integral coefficient  $K_i$  belong to DC voltage loop. Static gain is represented by  $s$ . The variation in DC voltage is represented by  $U_{dc}^*$ .  $U_{dc0}$  represents DC capacitor voltage reference and  $U_{dc}$  represents measured voltage of DC capacitor. Voltage deviation at DC link can be expressed as (6).

$$U^*_{dc} = \frac{1}{D_p}(\omega_g - \omega_o) \tag{6}$$

where  $D_p$  denotes the droop coefficient of DC voltage,  $\omega_g$  represents actual angular velocity of grid and  $\omega_o$  represents rated angular velocity of grid.

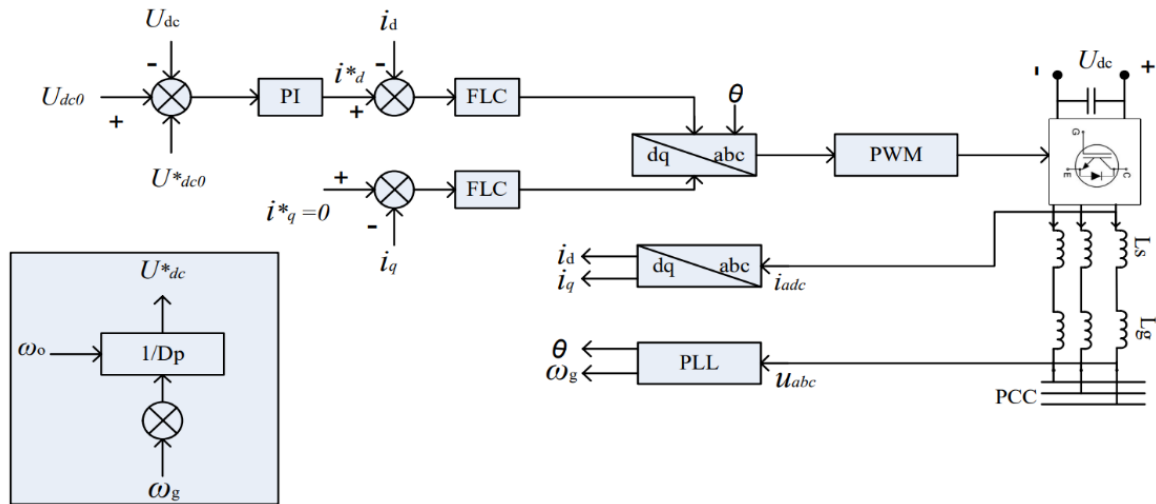


Figure 3. Grid-connected inverter control scheme

### 3. DYNAMIC CHARACTER ANALYSIS OF A GRID-CONNECTED PV POWER GENERATION SYSTEM

In this section dynamic characteristics of grid tied PV power system will be analyzed and influential function will be summarized. Results are then used to analyze the inertia, damping and synchronous dynamic performance of grid connected PV power generation system. The method of analyzing static stability and instability mechanism of rotational synchronous generator (RSG) system was given in and the dynamic process of grid-tied inverter under DC voltage control time scale is derived as (7):

$$\begin{cases} \frac{d \Delta \delta}{dt} = \Delta \omega \\ 2H \frac{d \Delta U_{dc}}{dt} = \Delta P_{in} - \Delta P_e \end{cases} \tag{1}$$

where power angle of the grid is denoted by  $\delta$ , while  $\omega$  denotes the angular frequency. Voltage on the capacitor's DC side is denoted by symbol  $U_{dc}$ .

The power that is fed into the energy transfer medium is denoted by  $P_{in}$ .  $P_e$  is output power of system, and  $H$  is inertial time constant that system possesses. After rewriting (7) into standard torque equation we get:

$$\begin{cases} \frac{d \Delta \delta}{dt} = \Delta \omega \\ T_j \frac{d \Delta \omega}{dt} = -T_d \Delta \omega - T_s \Delta \delta \end{cases} \tag{2}$$

where  $T_j$  is coefficient of inertia,  $T_d$  is damping coefficient, and  $T_s$  is synchronous coefficient of the SSG model. These three characteristics are deployed in conventional stability theory to characterize the dynamic behaviour of an SSG system. Analysis of electrical torque using the parameters  $T_j, T_d$ , and  $T_s$  provides information about the inverter system's capacity to mitigate inertia and achieve grid synchronization.

Grid-tied inverter's transient behavior is analyzed with the help of the SSG model before the inverter is put into service. Single phase simplified circuit diagram for grid connected inverter is given in Figure 4. Terminal voltage of grid-connected inverter is denoted by  $U_g$ , amplitude of the grid-tied inverter excitation potential is denoted by  $U_s$ . Difference between the grid-tied inverter and grid voltage is denoted by  $\delta$ .

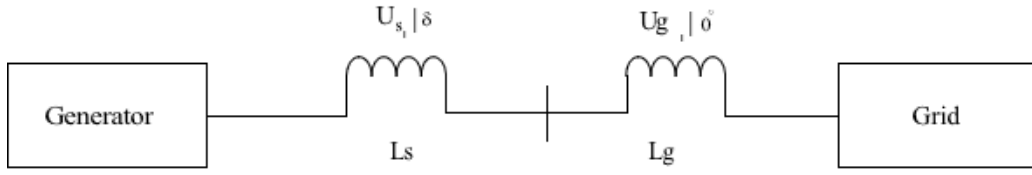


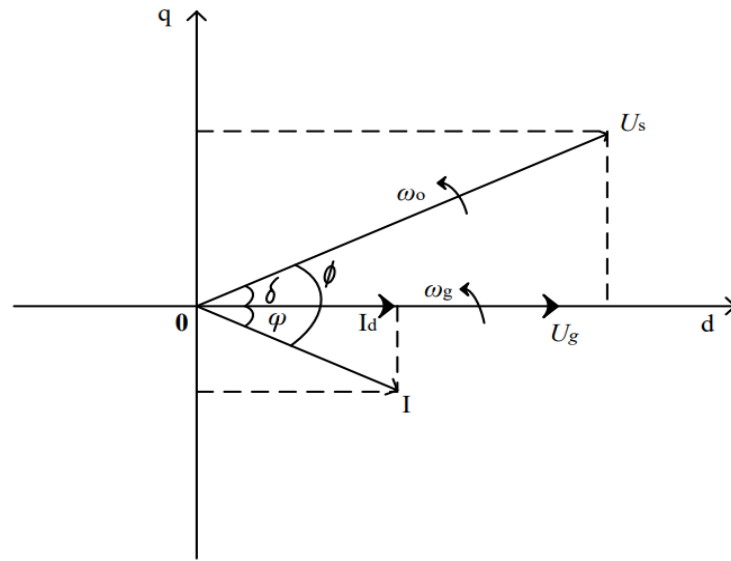
Figure 4. Single-phase grid-connected inverter

When analyzing and modelling grid-connected inverter systems, it is common practice to have the system be driven in relation to the grid voltage. The grid-tied inverter's vector diagram, with zero-line impedance and grid voltage assumed, is shown in Figure 5. Active power and active current output by the three-phase grid-connected inverter can be calculated by (9) and (10).

$$P_e = \frac{3}{2} \frac{U_s U_g}{X} \sin \delta \quad (3)$$

$$I_d = \frac{U_s}{X} \sin \delta \quad (4)$$

where  $X$  is a fixed inductance that is identical to that of the grid. All the above data was used as theoretical analysis in developing SSG model of grid tied PV system based on DC voltage droop control. This helps in analyzing the inertia, damping, and synchronization characteristics of grid-Connected PV power systems.

Figure 5. Vector representation in  $dq$  system

These techniques provide the theoretical foundation necessary to create an SSG model of the proposed method, complete with DC-side voltage control over the controlling droop. By incorporating (6) in (5) we get:

$$I_d = \left[ \frac{1}{D_p} (\omega_g - \omega_o) + U_{dco} - U_{dc} \right] \left( K_p + \frac{K_i}{s} \right) \quad (5)$$

By combining (10) and (11) we get:

$$\frac{U_s}{X} \sin \delta = - \left[ \frac{1}{D_p} (\omega_g - \omega_o) + U_{dco} - U_{dc} \right] \left( K_p + \frac{K_i}{s} \right) \quad (6)$$

The relation between variables is taken in case of small disturbances for the stability analysis and (12) can be linearized to (13).

$$sK\Delta\delta = -(sK_p + k_i) \left( \frac{1}{D_p} \Delta\omega - \Delta U_{dc} \right) \quad (7)$$

where power angle of the grid is denoted by  $\delta$  and  $K$  is defined in (14) as:

$$K = \frac{3}{2} \frac{U_s}{X} \cos\delta_o \quad (8)$$

linearization of (9) is:

$$\Delta P_e = \frac{3}{2} \frac{U_s U_g}{X} \cos\delta_o \Delta\delta \quad (9)$$

By incorporating (4) and (15) into (7), we can obtain the expression for voltage increment as (16).

$$\Delta U_{dc} = -\frac{3KU_g}{4H_s} \Delta\delta \quad (10)$$

The grid-integrated PV system's inertia and damping properties can be analyzed using the current AC torque approach. By using (16) to (13), we are eliminating the voltage increment. This leads to the following derivation of the SSG model for the grid-connected PV system using control of DC voltage droop by formation of standard electric torque (8):

$$\begin{cases} \frac{d\Delta\delta}{dt} = \Delta\omega \\ 2H \frac{K_p}{D_p} \frac{d^2\Delta\omega}{dt^2} + \left( 2HK + 2H \frac{K_i}{D_p} \right) \frac{d\Delta\omega}{dt} \\ = -\frac{3}{2} KU_g K_p \Delta\omega - \frac{3}{2} KU_g K_i \Delta\delta \end{cases} \quad (11)$$

The rate of frequency (RoCoF) [4], which measures how much the grid frequency changes during actual grid operation, is typically quite low. RoCoF's quadratic term in (17) can therefore be viewed as a high order an insignificant portion and can be ignored. Consequently, in (18) we have:

$$2H \left( K + \frac{K_i}{D_p} \right) \frac{d\Delta\omega}{dt} = -\frac{3}{2} KU_g K_p \Delta\omega - \frac{3}{2} KU_g K_i \Delta\delta \quad (12)$$

Comparing (17) with (8), from (19) we can determine the equivalent inertia parameter  $T_j$ , damping parameter  $T_d$ , synchronization parameter  $T_s$  i.e.:

$$\begin{cases} T_j = 2HK + 2 \frac{HK_i}{D_p} \\ T_d = \frac{3}{2} KU_g K_p \\ T_s = \frac{3}{2} KU_g K_i \end{cases} \quad (13)$$

Some examples of these significant properties under steady-state conditions are the power angle and the DC-side capacitance. Most effective and flexible way to include a PV system is by the process of adjusting the frequency that is coupled to the grid and to adjust the inverter control parameters. Equation (19) demonstrates that equivalent inertia coefficient  $T_j$  is affected by both droop coefficient  $D_p$  and proportional integral coefficient  $K_i$  of system's moment of inertia.

The ratio coefficient  $K_p$  of outer DC voltage control loop affects the system's equivalent damping coefficient  $T_d$ . Larger  $K_p$ , larger  $T_d$ , and stronger damping effect of the system.  $K_i$ , the proportional integral coefficient, derived from the outer DC voltage loop, influences  $T_s$  which is the synchronization coefficient. The greater the inertia of the system, the larger the DC voltage drop caused by the coupling between the DC voltage and the grid frequency. The outer DC voltage control loop's proportional coefficient  $K_p$  affects the damping, which in turn affects the deviation law. As the amount of deviation increases, so does the damping effect of the system. Efficiency with which the system may be synchronised increases as proportional integral coefficient  $K_i$  of the DC voltage outer loop increases.

#### 4. FUZZY LOGIC CONTROLLER

Fuzzy logic controllers (FLCs) have gained prominence in microgrid control due to their ability to handle complex nonlinear relationships and uncertainties inherent in microgrid operation. The effectiveness of FLCs depends on the establishment of well-defined and appropriate fuzzy rules. These rules form the core of the fuzzy control strategy, translating system inputs into control outputs.

In a microgrid context, fuzzy rules are typically formulated based on a combination of expert knowledge, system dynamics, and historical data analysis. The process of rule establishment involves identifying key input variables, defining membership functions for each variable, and establishing fuzzy relationships between inputs and outputs. Fuzzy controllers employ fuzzy logic to make decisions using incomplete or unclear data. FLCs have a fuzzifier, inference engine, rule basis, and defuzzifier.

Fuzzy sets are used with fuzzy logic operators in the inference engine to provide a fuzzy result. The term “fuzzification” refers to the process of decomposing information at the input or output of a system. While membership functions can take the form of any curve or table, the most common shapes are triangles and trapezoids because they are easier to represent in embedded controllers. To assess the measurable values, we create a fuzzy rule-based expert system. When assessing the value of an organization's intellectual property, a fuzzy linguistics approach will help in making more accurate decisions.

Aggregation is process of compiling all fuzzy sets which represent the results of each rule into single set. Before the last defuzzification process, all output variables are aggregated once. The result of an aggregated fuzzy set can be simplified to a single number using a technique called defuzzification. It is used to make an inference's fuzzy outcomes clearer. To achieve defuzzification, a decision-making algorithm is used to pick the most appropriate crisp value from a set of fuzzy solutions.

The crisp output is achieved by first reducing the combined fuzzy set to a single numerical value. Common defuzzification strategies include the center of mass method, the maximum method, and the mean of maximum method. Mamdani and Sugeno are two approaches to building fuzzy interface systems. The output of the Mamdani method must be represented as fuzzy sets. Instead of using several fuzzy sets, which can become tedious, it may be more convenient to employ a single relationship purpose of a linguistic variable.

The Singleton output mechanism is a method that reduces the amount of processing needed in the de-fuzzification process. whereas the Sugeno technique can be applied to the modelling of any inference system with a linear or constant membership function at its output. Similar to the Mamdani method [24], the first two phases of the Sugeno technique involve fuzzifying inputs and applying fuzzy operator.

With  $x$  and  $y$  represent the inputs,  $K$ ,  $L$ , and  $M$  are constants, the Sugeno method's output can be expressed as written as  $O = Kx + Ly + M$ . The resultant  $O$  of a zero-order Sugeno model is always the same ( $K = L = M$ ). Only the relative significance of each rule's command can determine its result. When comparing the effectiveness of Mamdani and Sugeno models, the Sugeno method provides better results [25].

For the proposed fuzzy controller, eigenvalues or impedance-based frequency domain techniques could offer a rigorous assessment of stability. Eigenvalue analysis involves computing the eigenvalues of the system matrix associated with the controller, ensuring that they all have negative real parts to confirm stability. On the other hand, impedance-based frequency domain analysis assesses the system's response to different frequencies of input signals, providing insights into stability characteristics across a range of operating conditions.

In the context of fuzzy control systems, eigenvalue analysis plays a crucial role in evaluating the ability of fuzzy controllers to maintain stability in complex and uncertain environments like microgrids. Eigenvalue analysis can be applied to fuzzy controllers by considering the fuzzy controller as an integral part of the overall system dynamics. The state equation of the system, which encapsulates the system's behavior, is augmented with the fuzzy controller's control rules and membership functions. By incorporating these analyses into the evaluation of the proposed fuzzy controller, the paper can substantiate its claim of stability, providing a more robust and comprehensive validation of the controller's performance in the specified application.

Figure 6 serves as the graphical representation of the complicated flowchart detailing the fuzzy logic controller employed in this study. The DC voltage droop control methodology is an intricate process encompassing several crucial components, including the formulation of the problem, determination of inputs and outputs, establishment of linguistic variables and their corresponding fuzzy sets, definition of membership functions, construction of rules, the transformation of inputs into fuzzy logic values, rule application, and ultimately, the process of de-fuzzifying the output variable. This comprehensive approach underscores the sophistication and precision involved in managing DC voltage droop through the application of FLC principles.



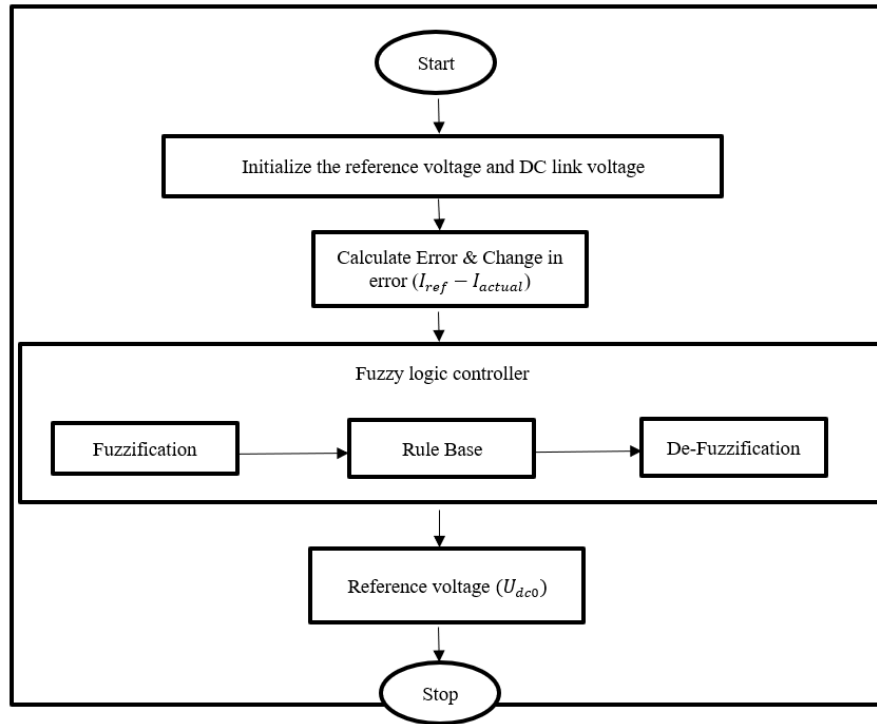


Figure 6. Flow chart of FLC

This methodology adeptly manages DC voltage droop, ensuring the uninterrupted operation of a grid-tied PV power generation system, even in the face of grid disturbances and fluctuations in solar irradiation levels. Figures 7 to 9, presented herein, respectively depict the error function, the rate of change in error, and the output membership function, encapsulating the intricate dynamics at play in this precise control mechanism.

Establishing fuzzy controller rules involves identifying key input and output variables like voltage error and control action, defining membership functions like “negative big” and “negative small”. Next, “IF-THEN” rules are constructed to capture expert knowledge or desired control strategies. These rules form the core of the fuzzy decision-making process. For example, a rule might state, “IF voltage error is negative large AND change in error is positive small, THEN increase duty cycle by a medium amount.” These rules map to inverter operations by addressing different conditions like load variations and indirectly influencing design parameters through control actions. Maintaining stability requires careful rule design to avoid oscillations, with analysis techniques like Lyapunov stability ensuring robustness. Tuning membership functions and rule weights might be needed to optimize performance and stability.

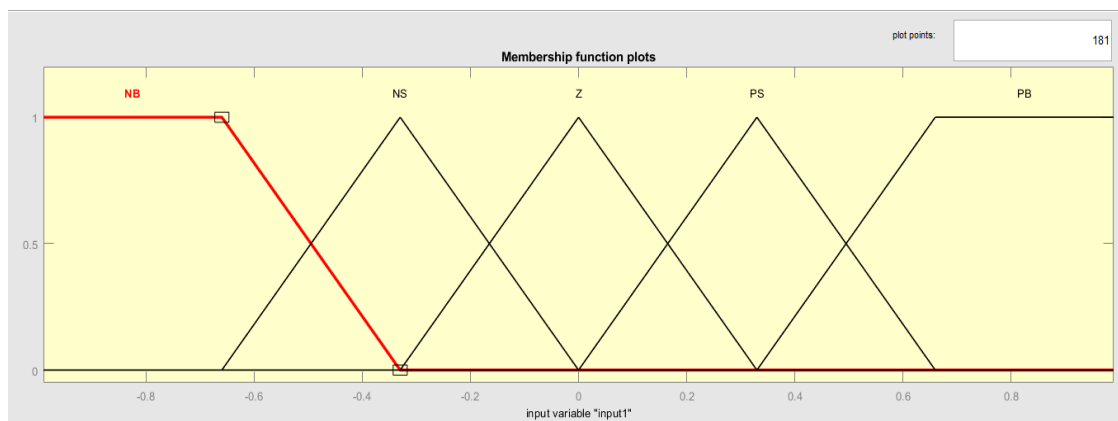


Figure 7. Input 1

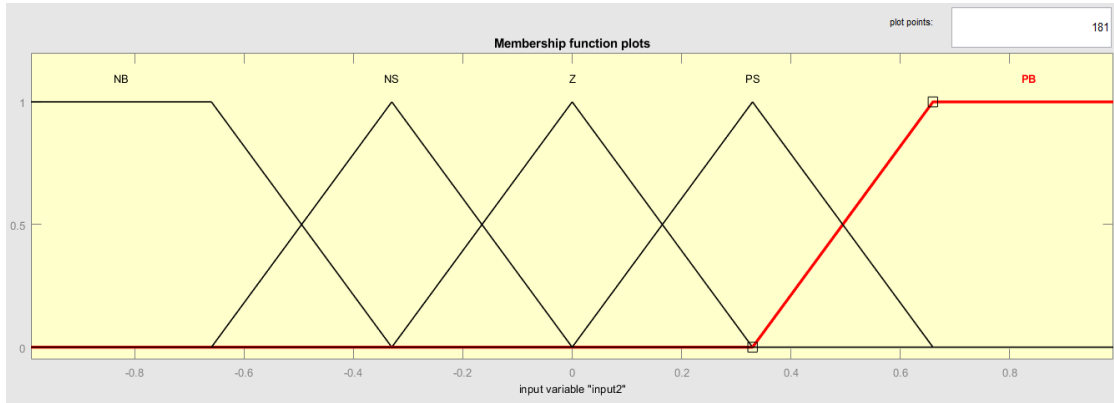


Figure 8. Input 2

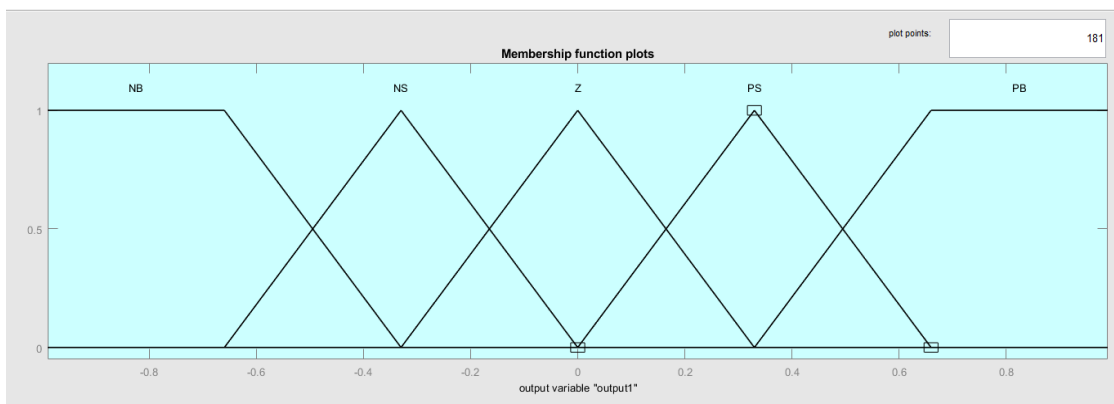


Figure 9. Output

Table 1 contains an explanation of the FLC regulations that were applied to this study along with list of critical simulation circuit parameters were given in Table 2. Where the inputs of the system are error ( $E$ ), change in error ( $\delta E$ ) and output is change in duty cycle ( $\delta D$ ). The process converts input and output variables of real crisp variables to fuzzy variables that were expressed by linguistic terms such as negative big (NB), negative small (NS), zero (Z), positive small (PS), and positive big (PB) of above mentioned 25 fuzzy IF-Then rules.

Table 1. FLC rules

$\Delta D$	$\Delta E$				
	NB	NS	Z	PS	PB
$E$	NB	PB	PS	PS	Z
	NS	PB	PS	Z	NS
	Z	PS	Z	NS	NS
	PS	PS	Z	NS	NB
	PB	Z	NS	NB	NB

Table 2. Parameters of the system

Factor	Value
Capacitance at DC bus /mF	5
PV side bus capacitance / $\mu$ F	100
Filter Inductance at DC side /mH	24
Voltage at Dc side /v	750
Line-line voltage of grid /V	380
Inductance of filter /mH	3
Frequency at grid /Hz	50
Reactance related to line /mH	0.5

## 5. SIMULATION RESULTS

The process would involve assessing the efficiency of FLC in PV systems as shown in Figure 1 using MATLAB/Simulink 2018a. When in the simulation, operating condition is set to  $t = 1$  s, the grid frequency decreases by 0.2 Hz. This is because frequency deviations can occur due to sudden changes in load, faults in the grid, or fluctuations in power generation from sources like PV systems, which may require grid control mechanisms to restore the desired frequency level. Simulation results show the effect of system parameters on inertia, damping and synchronization characteristics.

### 5.1. Droop mechanism analysis

Figures 10 and 11 shows the simulations of a grid-connected PV system with and without droop loop, respectively. It shows the effect of frequency deviation to form the dc voltage droop on the system. Despite fluctuations in grid frequency, the DC/DC converter maintains a constant power output and DC voltage for the system.

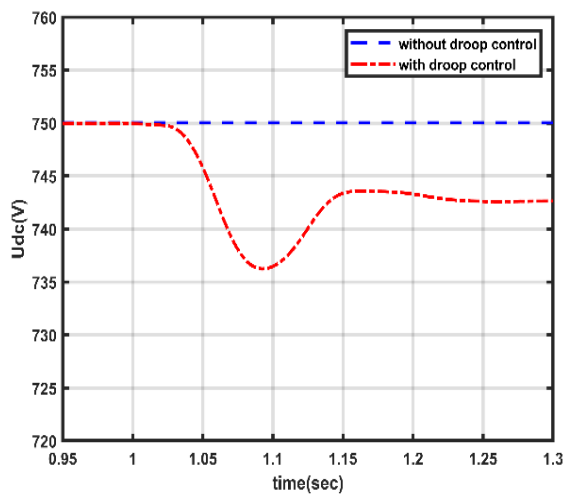


Figure 10. Effect of various parameter changes on system inertia

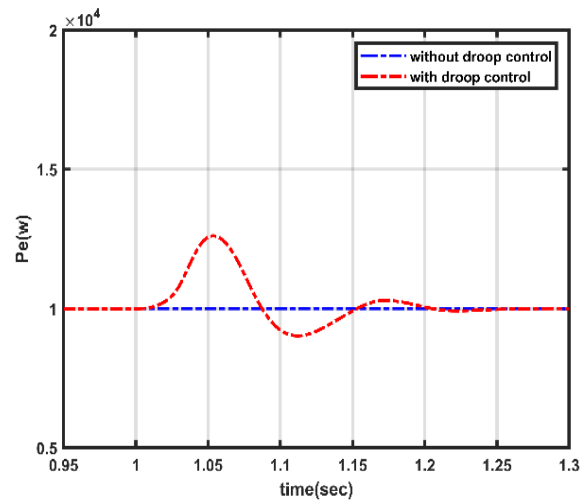


Figure 11. Effect of various parameter changes on system power

Frequency deviation is introduced to establish the droop loop, however, DC-side capacitor begins to react to changes in grid's frequency. By decreasing grid frequency, capacitor's side voltage will decrease when energy is discharged, allowing the system to produce more power. When operating with droop control, the system allows the DC voltage ( $U_{dc}$ ) to vary with time, due to the use of a droop control strategy. Droop control adjusts the voltage level based on the load demand and power. This variation helps to maintain stable system operation and balance power supply and demand, ensuring efficient energy distribution within the microgrid. Droop control offers adaptability and stability by allowing voltage variations. When the system is operating in without droop condition, the system maintains a constant DC voltage and other mechanisms, such as voltage regulators or power electronics, are used to maintain the voltage at a set value. Without droop control, the system may not adapt as dynamically to changes in load or power generation and may require more active control to maintain voltage stability. This system depends on additional control mechanisms to maintain constant voltage levels and may face challenges in responding to rapid changes in load or generation.

### 5.2. Analysis of inertia characteristics by using PI and FLC

DC voltage droop control is used to design a PV system connected to the grid by keeping  $K_p$  and  $K_i$  constant. DC-side capacitor voltage is found to oscillate more strongly as  $1/D_p$  is increased. Controlling the voltage drop is crucial for maintaining a constant oscillation amplitude. The results of this performance analysis of the system are shown in Figures 12 and 13, which indicate the various ranges that were used. The following results had been obtained using a FLC for the various values of  $1/D_p$ , such as 60, 80, and 100. The results of  $U_{dc}$  for the above-mentioned values were obtained at different trough values such as 741, 737, and 734.5 V, respectively after being enhanced. In the same way, the change in  $P_e$  had been observed from different trough values at 9.5, 10, and 10.5 kW for the same  $1/D_p$  values. This results shows the

improvement to existing PI controller which can be referred in [26]. The FLC adjusts its control settings dynamically as  $1/D_p$  increases, thereby increasing voltage oscillations and tuning active power control. Finally, this shows that greater the  $1/D_p$ , stronger will be the inertia characteristics of the system. Thereby showing better inertia characteristic performance of system when compared by PI controller.

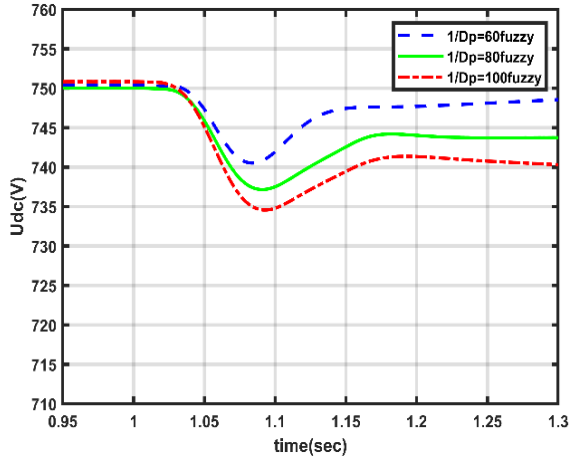


Figure 12. Effect of droop co-efficient  $D_p$  on system voltage

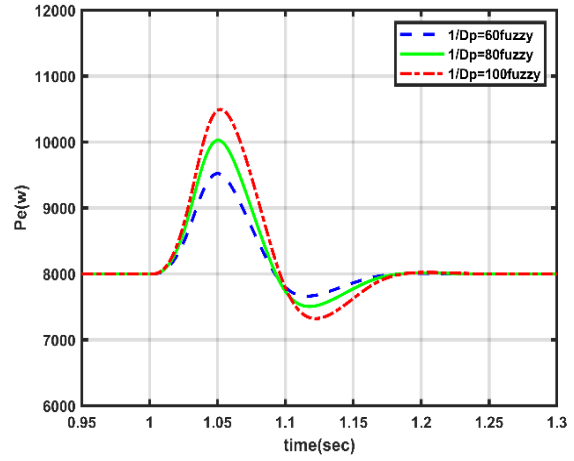


Figure 13. Effect of droop co-efficient  $D_p$  on system power

### 5.3. Analysis of damping characteristics by using PI and FLC

In simulation of grid-connected PV system regulated via droop control of DC voltage observed a change in damping qualities of the system by changing the  $K_p$ . while  $1/D_p$  and  $K_i$  were held constant. The results of the performance analysis of the system are shown in Figures 14 and 15. The following results had been obtained using a FLC for the various values of  $K_p$ , such as 0.5, 0.7, and 0.9. The results of  $U_{dc}$  for the above-mentioned values were obtained at different trough values such as 733, 735, and 737 V respectively by using FLC. In the same way, the change in  $P_e$  had been observed from different trough values at 14.5, 13, and 12 kW for the same  $K_p$  values. The improvement in system performance from the existing PI controller to the FLC is due to the fuzzy controller's adaptability. When we change  $K_p$  values, the FLC adjusted its control parameters, which reduced voltage fluctuations and improved active power control. This adaptability allowed the fuzzy controller to keep voltage ( $U_{dc}$ ) more stable and regulate active power ( $P_e$ ) more accurately. On the other hand, the PI controller could not adapt as effectively to changing control parameters, leading to less stable  $U_{dc}$  and less precise  $P_e$  regulation.

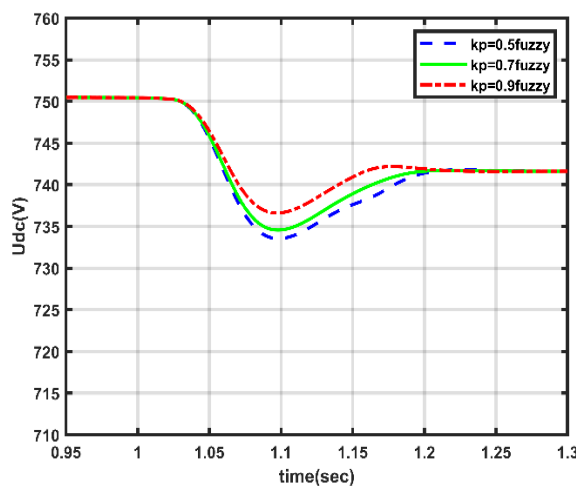


Figure 14. Effect of  $P$  controller on system voltage

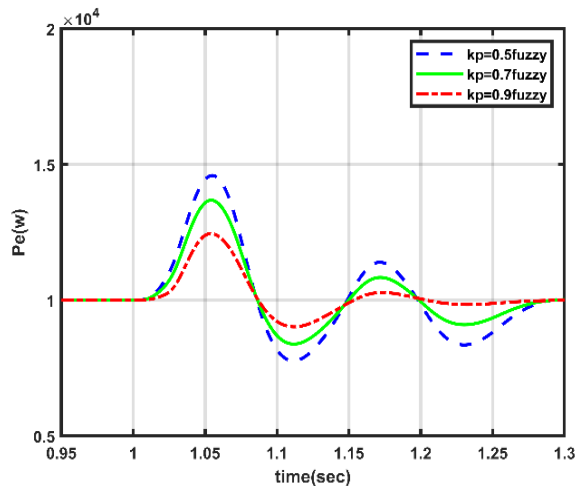


Figure 15. Effect of  $P$  controller on system power

When  $K_p$  of the system is larger, then amplitude of the DC side capacitor voltage drop will be smaller and thereby smaller will be amplitude of the voltage and power oscillations. Finally, larger  $K_p$ , stronger the damping effect of the system. This results shows improvement to the already-existing PI controller, which can be referred to in [26].

#### 5.4. Analysis of synchronization characteristics using PI and FLC

Both  $K_p$  and  $1/D_p$  were remained steady during the simulation of a PV system connected to the grid. The results of the performance analysis of the system are shown in Figures 16 and 17. The following results had been obtained using a FLC for the various values of  $K_i$ , such as 0.5, 0.7 and 0.9. The results of  $U_{dc}$  for the above-mentioned values were obtained at different trough values such as 726, 728, and 730 V respectively. In the same way, the change in  $P_e$  had been observed from different trough values at 17, 16, and 14 kW for the same  $K_i$  values. When we adjust  $K_i$  values, the FLC tuned its control parameters, resulting in reduced voltage fluctuations and enhanced active power control.

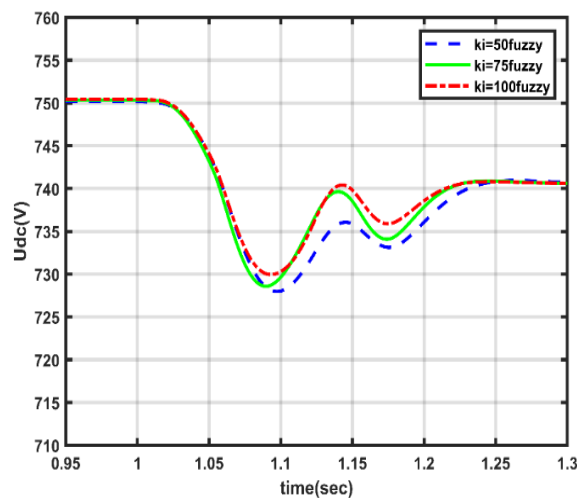


Figure 16. Effect of  $I$  controller on system voltage

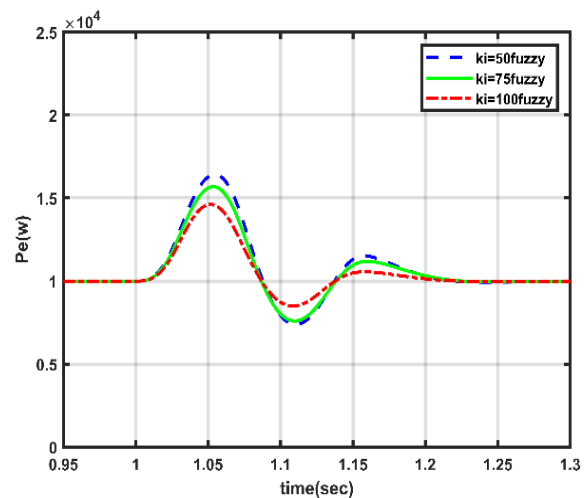


Figure 17. Effect of  $I$  controller on system power

When compared with system which is having PI controller [26] results are far better when using FLC. This shows that changes in  $K_i$  have a greater effect on the properties of synchronization. This flexibility allowed the fuzzy controller to maintain a more stable voltage ( $U_{dc}$ ) and achieve more accurate active power ( $P_e$ ) regulation. On the other hand, the PI controller lacked this adaptability, which led to less effective performance when control parameters changed. In conclusion, when the system is having larger  $K_i$ , then the system will be having stronger synchronization characteristics. Above all results showed that FLC surpasses traditional proportional-integral (PI) controllers in grid-connected photovoltaic systems, offering enhanced inertia characteristics, synchronization, and reduced oscillations. FLCs, with their ability to handle uncertainty through linguistic variables, prove superior in optimizing system performance and stability, making them the preferred choice for efficient renewable energy integration.





## 6. CONCLUSION

In grid-connected photovoltaic systems, the implementation of FLC has made it feasible to make significant improvements in terms of both performance and total system stability. By utilizing an FLC, more precise and dynamic control of the DC voltage drop can be achieved. In the present study, by replacing the existing PI controller with FLC, the effect of  $K_p$ ,  $K_i$  and  $D_p$  were carried out on the following characteristics: inertia, damping and synchronization to analyze the system performance. It can be concluded from simulation results that the inertia characteristics of system is stronger if  $1/D_p$  is larger. Similarly, the larger value of  $K_p$  and  $K_i$ , the stronger will be the damping and synchronization characteristics of the system. Finally, from simulation it is clearly observed that the FLC is superior to the PI control in terms of the overall performances of inertia, damping and synchronization characteristics. This paper provides important information on the possibilities of employing FLC in grid-connected photovoltaic systems, which has the potential to significantly improve the stability of such systems when facing minor disruptions.





## REFERENCES

- [1] S. R. Sinsel, R. L. Riemke, and V. H. Hoffmann, "Challenges and solution technologies for the integration of variable renewable energy sources—a review," *Renewable Energy*, vol. 145, pp. 2271–2285, 2020, doi: 10.1016/j.renene.2019.06.147.
- [2] B. A. Taye and N. B. D. Choudhury, "A dynamic droop control for a DC microgrid to enhance voltage profile and proportional current sharing," *SSRN Electronic Journal*, vol. 221, no. April, 2022, doi: 10.2139/ssrn.4268907.
- [3] S. Tan, Q. Lv, H. Geng, and G. Yang, "An equivalent synchronous generator model for current-controlled voltage source converters considering the dynamic of phase-locked-loop," in *IECON Proceedings (Industrial Electronics Conference)*, 2016, pp. 2235–2240, doi: 10.1109/IECON.2016.7792983.
- [4] J. Hu, Y. Lei, Y. Chi, and X. Tian, "Analysis on the inertia and the damping characteristics of DFIG under multiple working conditions based on the grid-forming control," *Energy Reports*, vol. 8, pp. 591–604, 2022, doi: 10.1016/j.egyr.2022.09.200.
- [5] W. Binbing, X. Abudwayiti, C. Yuxi, and T. Yizhi, "RoCof droop control of PMSG-based wind turbines for system inertia response rapidly," *IEEE Access*, vol. 8, pp. 181154–181162, 2020, doi: 10.1109/ACCESS.2020.3027740.
- [6] M. Rodriguez, V. Espin, D. Arcos-Aviles, and W. Martinez, "Energy management system for an isolated microgrid based on fuzzy logic control and meta-heuristic algorithms," *IEEE International Symposium on Industrial Electronics*, pp. 462–467, 2022, doi: 10.1109/ISIE51582.2022.9831553.
- [7] H. Tekin, K. Bulut, and D. Ertekin, "A novel switched-capacitor and fuzzy logic-based quadratic boost converter with mitigated voltage stress, applicable for DC micro-grid," *Electrical Engineering*, vol. 104, no. 6, pp. 4391–4413, 2022, doi: 10.1007/s00202-022-01631-3.
- [8] K. A. Al Sumarmad, N. Sulaiman, N. I. A. Wahab, and H. Hizam, "Energy management and voltage control in microgrids using artificial neural networks, PID, and fuzzy logic controllers," *Energies*, vol. 15, no. 1, 2022, doi: 10.3390/en15010303.
- [9] A. Mahrouch and M. Ouassaid, "Primary frequency regulation based on deloaded control, ANN, and 3D-fuzzy logic controller for hybrid autonomous microgrid," *Technology and Economics of Smart Grids and Sustainable Energy*, vol. 7, no. 1, 2022, doi: 10.1007/s40866-022-00125-2.
- [10] J. Xiao, Y. Jia, B. Jia, Z. Li, Y. Pan, and Y. Wang, "An inertial droop control based on comparisons between virtual synchronous generator and droop control in inverter-based distributed generators," *Energy Reports*, vol. 6, pp. 104–112, 2020, doi: 10.1016/j.egyr.2020.12.003.
- [11] S. D'Arco and J. A. Suul, "Equivalence of virtual synchronous machines and frequency-droops for converter-based Microgrids," *IEEE Transactions on Smart Grid*, vol. 5, no. 1, pp. 394–395, 2014, doi: 10.1109/TSG.2013.2288000.
- [12] K. M. Cheema *et al.*, "Virtual synchronous generator: modifications, stability assessment and future applications," *Energy Reports*, vol. 8, pp. 1704–1717, 2022, doi: 10.1016/j.egyr.2021.12.064.
- [13] L. Xiong, X. Liu, Y. Liu, and F. Zhuo, "Modeling and stability issues of voltage-source converter-dominated power systems: a review," *CSEE Journal of Power and Energy Systems*, vol. 8, no. 6, pp. 1530–1549, 2022, doi: 10.17775/CSEEJPES.2020.03590.
- [14] H. Yuan, X. Yuan, and J. Hu, "Modeling of grid-connected VSCs for power system small-signal stability analysis in DC-link voltage control timescale," *IEEE Transactions on Power Systems*, vol. 32, no. 5, pp. 3981–3991, 2017, doi: 10.1109/TPWRS.2017.2653939.
- [15] P. Saxena, N. Singh, and A. Kumar Pandey, "Enhancing the transient performance and dynamic stability of microgrid using PI inertia injection controller," *International Journal of Electrical Power and Energy Systems*, vol. 134, Jan. 2022, doi: 10.1016/j.ijepes.2021.107334.
- [16] D. Chethan Raj and D. N. Gaonkar, "Frequency and voltage droop control of parallel inverters in microgrid," in *2016 2nd International Conference on Control, Instrumentation, Energy and Communication*, 2016, no. 3, pp. 407–411, doi: 10.1109/CIEC.2016.7513771.
- [17] L. Xiong *et al.*, "Static synchronous generator model: a new perspective to investigate dynamic characteristics and stability issues of grid-tied PWM inverter," *IEEE Transactions on Power Electronics*, vol. 31, no. 9, pp. 6264–6280, 2016, doi: 10.1109/TPEL.2015.2498933.
- [18] T. Hai, J. Zhou, and K. Muranaka, "An efficient fuzzy-logic based MPPT controller for grid-connected PV systems by farmland fertility optimization algorithm," *Optik*, vol. 267, 2022, doi: 10.1016/j.jjleo.2022.169636.
- [19] J. Hmad, A. Houari, H. Trabelsi, and M. Machmoum, "Fuzzy logic approach for smooth transition between grid-connected and stand-alone modes of three-phase DG-inverter," *Electric Power Systems Research*, vol. 175, 2019, doi: 10.1016/j.epr.2019.105892.
- [20] J. Fang, H. Li, Y. Tang, and F. Blaabjerg, "Distributed power system virtual inertia implemented by grid-connected power converters," *IEEE Transactions on Power Electronics*, vol. 33, no. 10, pp. 8488–8499, 2018, doi: 10.1109/TPEL.2017.2785218.
- [21] V. Kumar, A. S. Pandey, and S. K. Sinha, "Grid integration and power quality issues of wind and solar energy system: a review," *International Conference on Emerging Trends in Electrical, Electronics and Sustainable Energy Systems*, vol. 2011, pp. 71–80, 2016, doi: 10.1109/ICETESES.2016.7581355.
- [22] Y. Zha, J. Lin, G. Li, Y. Wang, and Yizhang, "Analysis of inertia characteristics of photovoltaic power generation system based on generalized droop control," *IEEE Access*, vol. 9, pp. 37834–37839, 2021, doi: 10.1109/ACCESS.2021.3059678.
- [23] D. Wang, L. Xiong, and J. Lin, "An inertia emulation method based on improved double-loop control for grid-tied inverters," in *2017 IEEE 3rd International Future Energy Electronics Conference and ECCE Asia, IFEEC - ECCE Asia 2017*, 2017, pp. 2213–2217, doi: 10.1109/IFEEC.2017.7992395.
- [24] T. Samavat *et al.*, "A comparative analysis of the Mamdani and Sugeno fuzzy inference systems for MPPT of an islanded PV system," *International Journal of Energy Research*, vol. 2023, 2023, doi: 10.1155/2023/7676113.
- [25] M. A. Hartani, M. Hamouda, O. Abdelkhalek, and S. Mekhilef, "Sustainable energy assessment of multi-type energy storage system in direct-current-microgrids adopting Mamdani with Sugeno fuzzy logic-based energy management strategy," *Journal of Energy Storage*, vol. 56, 2022, doi: 10.1016/j.est.2022.106037.
- [26] F. Wu *et al.*, "Inertia and damping analysis of grid-tied photovoltaic power generation system with DC voltage drop control," *IEEE Access*, vol. 9, pp. 38411–38418, 2021, doi: 10.1109/ACCESS.2021.3059687.

**BIOGRAPHIES OF AUTHORS**

**Mimmithi Bhanu Prakash**     received the Bachelor of Technology (B.Tech.) degree in electrical and electronics engineering from Koneru Lakshmaiah University (KLU) in 2019. He received the Master of Technology (M.Tech.) degree in energy systems from Jawaharlal Nehru Technological University, Anantapur in 2022. Currently he is a research scholar at Vellore Institute of Technology – Andhra Pradesh (VIT-AP). His research interests include power systems, power electronics and renewable energy systems. He can be contacted at email: bhanuprakash18041998@gmail.com; Prakash.22phd7015@vitap.ac.in.



**Pradosh Ranjan Sahoo**     received the B.Tech. degree in electronics and telecommunication engineering from Biju Patnaik University of Technology, Rourkela, India in 2007, the M.Tech. degree in control and automation and Ph.D. degree from National Institute of Technology Rourkela, India in 2012 and 2019 respectively. He is now associated with the School of Electronics Engineering, VIT-AP University, Andhra Pradesh. His research interest includes decentralized control, robust control, and time delay systems. He can be contacted at email: pradosh.sahoo@vitap.ac.in.